EFFECT OF CALCINATION TEMPERATURE ON THE PHASE COMPOSITION AND MAGNETIC PROPERTIES OF THE BOEHMITE WITH ADSORBED FERROCENE

A.I. Rustamova[1], R.M. Muradkhanov[1], S.N. Osmanova[1,2], S.O. Soloviev[3], E.H. Ismailov[1]

[1]Institute of Catalysis and Inorganic Chemistry named after acad. M. Naghiyev, H.Javid Ave.,113, AZ 1143, Baku, Azerbaijan
[2]Khazar University, 41 Mahsati Str., AZ1096, Baku, Azerbaijan
[3]L.V. Pisarzhevskii Institute of Physical Chemistry of the National Academy of Sciences of Ukraine 31, Pr. Nauky, 03028, Kyiv, Ukraine
aygun.rustamova1601@gmail.com

Received 18.06.2024
Accepted 21.08.2024

Abstract: *The effect of calcination temperature in air of finely dispersed boehmite powders with ferrocene adsorbed at room temperature from n-hexane solution on X-ray diffraction patterns and EPR spectra of calcined samples was studied. It has been shown that calcination in air of boehmite samples with adsorbed ferrocene leads to the decomposition of ferrocene molecules, stabilization of two types of magnetic centers in the structure of boehmite (at 200 and 400°C) and aluminum oxide (at 600°C) caused by two types of magnetic centers -Fe^{3+} ions with g-factor values, equal to 4.3 and 2.0. The signal at g = 4.3 is attributed to isolated Fe^{3+} ions in the structure of boehmite and aluminum oxide in a local field of oxygen anions with a rhombic environment. The signal at g = 2.0 is most likely due to Fe^{3+} ions bound by dipole interaction for samples with a low concentration of supported ferrocene (<0.1 wt.%) and superpara/ferromagnetic FeOx particles for samples of the calcination product of boehmite with a high content (>0.1 wt.%) of ferrocene. With increasing content of adsorbeded ferrocene, concentrations of Fe^{3+} ions with g-factor values equal to 4.3 and 2.0 grow disproportionately, and mainly the growth of the concentration of superpara/ferromagnetic FeOx particles on the oxide surface is observed.*

Keywords: *Ferrocene, boehmite, calcination, XRD, EPR, TG/DTA*
DOI: 10.32737/2221-8688-2025-1-107-115

1. Introduction

Over the years since its discovery, ferrocene [$Fe(C_5H_5)_2$] has remained the focus of many research centers and is considered a promising material for potential use in various fields of science, technology, and medicine [1-4]. Two aromatic 5-membered cyclopentadienyl (Cp) rings coordinating iron in the oxidation state of +2 make ferrocene very stable. Due to its unique electronic and structural features, ferrocene and its derivatives have been used to synthesize a wide range of materials, including polymers, liquid crystals, and nanoparticles, with a variety of electronic and magnetic properties. Ferrocene is used as a potential electrode material in redox flow batteries due to its reversible redox behavior and high stability, as a lubricant to improve the performance and durability of engines and industrial equipment, and in the development of drugs for the treatment of cancer and many tropical diseases, in the creation of sensors, nanoscale magnetic materials, and in hydrogen storage [5-8]. Ferrocene is stable in air, characterized by low toxicity, low cost, and reversible redox properties. In the presence of oxidants, ferrocene is oxidized to ferrocenium cation [9, 10]. The discovery of ferrocene and its structural feature initiated an explosive revival of organometallic chemistry [11]. There is also an increased interest in adsorbed ferrocene and its derivatives, their chemistry on the surface of various solids [12]. The adsorption of ferrocene on metals and their oxides, zeolites, carbon materials - graphene (pure and functionalized), etc. has been studied [13-16]. It is indicated that ferrocene is adsorbed on solid surfaces with a

preferred orientation, which strongly depends on the substrate [17, 18]. Studies indicate physical adsorption of ferrocene with the Cp ring parallel to the surface on Ag(100), and with the Cp ring perpendicular to the Cu(100) surface [19]. Ferrocene is reported to dissociate upon physical adsorption on Au(III) at room temperature [20]. The adsorption behavior and geometry of the stabilized ferrocene molecule on graphene substrates have been investigated using density functional theory calculations taking into account van der Waals forces. These calculations showed that on graphene substrates (pure, oxygen- and hydroxyl-functionalized) the ferrocene molecule is adsorbed with the molecular axis parallel and perpendicular to the surface.

It should be noted that studies of the surface chemistry of ferrocene and its derivatives are just beginning to gain intensive attention [21, 22]. Studies show that ferrocene is a highly volatile substance and when heated to 170-180 °C it sublimates without decomposition. When the heating temperature increases to 400 °C, it decomposes in a stream of inert gas according to the scheme: $(C_5H_5)_2Fe \rightarrow Fe + H_2 + CH_4 + C_5H_6 + \ldots$. [23, 24] and upon calcination - according to the scheme: $2Fe(C_5H_5)_2 + 26.5O_2 = Fe_2O_3 + 20CO_2 + 10H_2O$ [25, 26].

This paper presents the results of a study of the effect of calcination of finely dispersed boehmite powders with ferrocene adsorbed at room temperature from an n-hexane solution on the phase composition and EMR spectra, and discusses the chemistry of the thermal decomposition of ferrocene adsorbed from an n-hexane solution into boehmite in an oxidizing environment in an air flow.

This paper presents the results of a study of the effect of calcination temperature of finely dispersed boehmite powders with ferrocene adsorbed at room temperature from an n-hexane solution on the phase composition and EPR spectra of the decomposition products, and also discusses the chemistry of the thermal decomposition of ferrocene adsorbed from an n-hexane solution into boehmite in an oxidizing environment in an air flow.

2. Experimental part

Ferrocene was obtained in laboratory conditions using the method described in [27] and characterized by elemental analysis, X-ray diffractometry, UV/Vis electronic absorption and FTIR spectroscopy. Fine boehmite powder produced by Qualikems, India was used as an oxide carrier. The boehmite powders with adsorbed ferrocene were obtained by applying n-hexane solutions of ferrocene with different concentrations to finely dispersed boehmite powders at room temperature, followed by drying at 50°C for 4 hours. Thus, samples of finely dispersed boehmite powders containing 0.1, 1.0, 4.8 and 13.04 wt.% of adsorbed ferrocene were obtained. Then these samples were divided into four equal parts and every three of the four parts were calcined in air for 4 hours at 200, 400 and 600 oC. Thermograms of the powder samples of boehmite with applied ferrocene were obtained using a STA 449 F3 Jupiter thermal analyzer from NETZSCH, Germany, in an air flow in the range of 25-900°C at a temperature rise rate of 10°C/min. The phase composition of boehmite powders with adsorbed ferrocene was determined by X-ray diffractometry using a Phaser D2 diffractometer, Bruker the infrared spectra of these samples were recorded on an FT-IR Alfa spectrometer and EPR spectra on an EMRmicro spectrometer, Bruker, Germany. UV/Vis spectra of the n-hexane solutions of ferrocene were obtained using Specord 50plus, UV/Vis spectrophotometer, Jena, Germany.

3. Results and discussion

Fig. 1, a, b show diffraction patterns of finely dispersed powders of boehmite and ferrocene dried at a temperature of 50 °C for 4 hours.

The observed diffraction patterns are characteristic of the boehmite phase γ-AlOOH (JCPD No. 21-1307) and the ferrocene compound (JCPD No. 00-029-1711), respectively.

Fig. 2 shows X-ray diffraction patterns recorded at room temperature of finely dispersed boehmite powders with ferrocene adsorbed at room temperature from an n-hexane solution, dried at a temperature of 50°C (a), and then calcined in air at 200 °C (b), 400 °C (c), and 600 °C (d).

As can be seen from the diffraction patterns shown in Fig. 2, the boehmite structure remains unchanged even for samples calcined in air at 400 °C for 2 hours. The crystalline structure of γ-AlOOH, described in [28], is orthorhombic. The unit cell consists of two double layers of distorted $AlO_4(OH)_2$ octahedra with an aluminum center. The OH groups are located on the outer surface of the double layers and interact, holding the layers together.

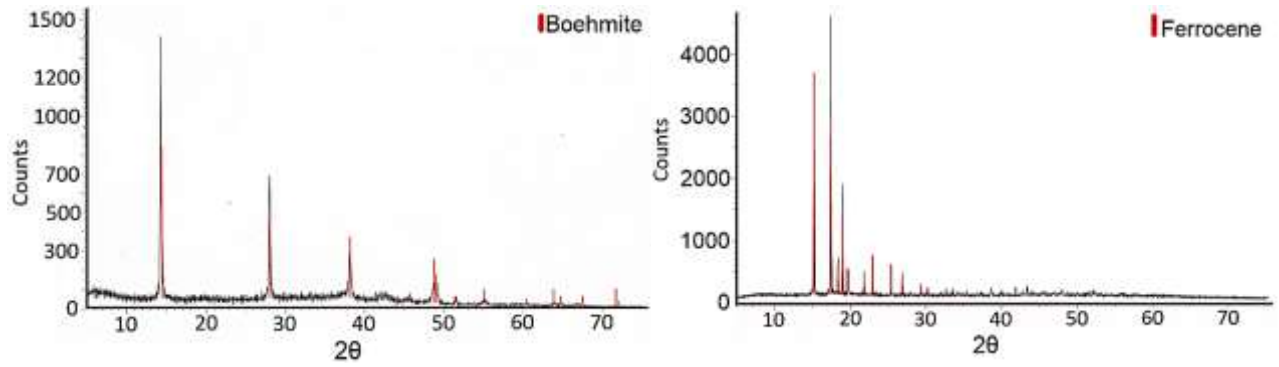

a) b)

Fig. 1. Diffraction patterns of finely dispersed powders of boehmite (a) and ferrocene (b) dried at a temperature of 50°C for 4 hours.

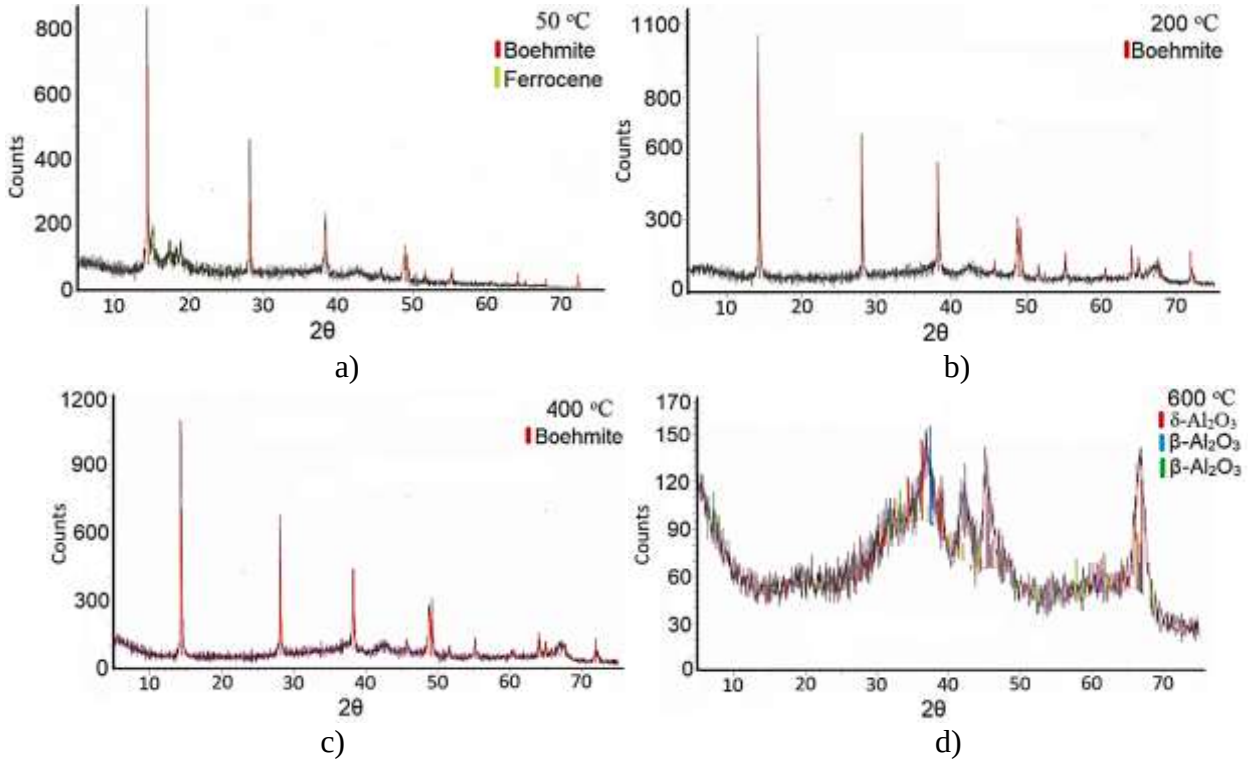

a) b)

c) d)

Fig. 2. X-ray diffraction patterns recorded at room temperature of finely dispersed boehmite powder with adsorbed ferrocene (13.0 wt.%) dried at 50°C (a) and then calcined in air at 200 °C (b), 400 °C (c), and 600 °C (d).

It is believed that in the boehmite crystal, half of the hydroxyls are interlayer and the other half are surface [29, 30]. For samples calcined at 600 °C, only phases characteristic of aluminum oxide are observed.

Fig. 3 shows the EPR spectra recorded at room temperature of finely dispersed boehmite powders dried at a temperature of 50°C (a) and then calcined in air for 2 hours at a temperature of 400 °C (b) and 600 °C (c).

As can be seen from the EPR spectrum shown in Fig. 3a, the finely dispersed boehmite sample used as a carrier contains impurity iron ions Fe^{3+}, stabilized in the boehmite structure in the form of isolated ions, replacing the Al^{3+} ions (the values of the radii of the Al^{3+} and Fe^{3+} ions are 0.53 and 0.62 A, respectively). The EPR spectrum of these ions is characterized by an almost symmetrical shape with a width of ~160 G and a g-factor value of 4.3.

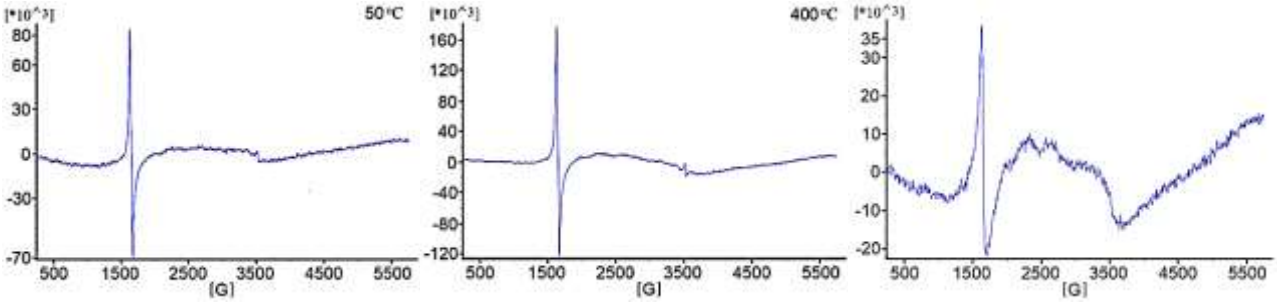

a) b) c)

Fig. 3. EPR spectra recorded at room temperature of finely dispersed boehmite powders dried at a temperature of 50°C (a) and then calcined in air for 2 hours at a temperature of 400 °C (b) and 600 °C (c).

We believe that the observed signals in Fig. 3.a,b are unusual, in the sense that not a single similar signal for iron ions in the boehmite structure has been found in the literature. The shape and position of these signals indicate that the Fe^{3+} ions are in octahedral fields with a high degree of distortion. For the heat treatment at 600 ^{o}C, it is noted that the signal around g = 2.0 increases significantly, while the signal with g = 4.3 decreases noticeably, indicating that the Fe^{3+} ions with signals near g = 2 are increased by Fe^{3+} with a g -factor of 4.3. The results of the XRD data (Fig. 2) show that the crystal structure of boehmite is unstable to the severe thermal-oxidative treatment at 600 ^{o}C. In this case, boehmite is transformed into aluminum oxide. Such thermal-oxidative treatment stimulates the rearrangement of Fe^{3+} ions and favors the formation of clusters from FeOx structures.

Fig. 4 shows the EPR spectra at room temperature of finely dispersed boehmite powder calcined in air at a temperature of 600 °C for 2 hours, containing (a) 0.1, (b) 1, (c) 4.8 and (d) 13.0 wt. % adsorbed ferrocene.

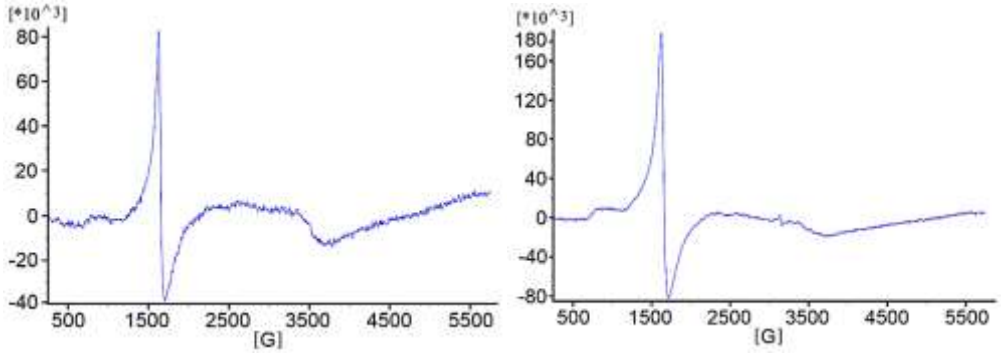

a) b)

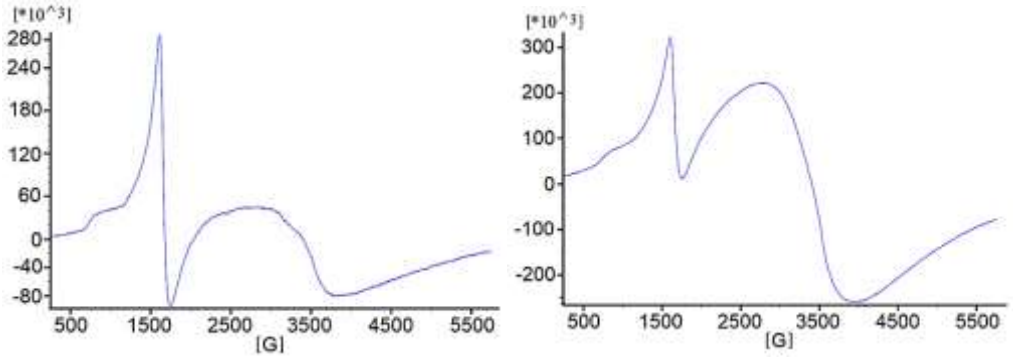

c) d)

Fig. 4. EPR spectra recorded at room temperature of finely dispersed boehmite powder with adsorbed ferrocene calcined in air at a temperature of 600 °C for 2 hours – (a) – 0.1, (b) – 1, (c) – 4.8 and (d) – 13.0 wt. % ferrocene.

As can be seen from the presented EPR spectra, two types of magnetic centers are observed. The first type most likely belongs to isolated iron ions Fe^{3+} with a g-factor value of 4.3 and stabilized in local fields of oxygen anions of distorted tetrahedral or octahedral shapes with rhombic distortion, and the second to clusters of Fe^{3+} ions bound by dipole-dipole and exchange interactions at low ferrocene contents (< 0.1 wt.%) and FeOx particles for samples with a higher ferrocene concentration (1.0-13.0 wt.%) [31, 32]. In this case, these two centers are formed during thermal decomposition in an oxygen atmosphere of ferrocene deposited on boehmite [33, 34]:

$$2(C_5H_5)_2Fe + 2AlO(OH) + 26.5O_2 \rightarrow Fe_2O_3 + Al_2O_3 + 11H_2O + 20CO_2 \qquad (1)$$

The mass of the solid residue in accordance with this equation of decomposition of ferrocene deposited on boehmite is 19.0 wt.%.

Fig. 5 shows thermograms of finely dispersed boehmite powders with ferrocene adsorbed at room temperature from an n-hexane solution, containing 0.1 and 13.0 wt.% ferrocene and dried at 60 °C for 2 hours.

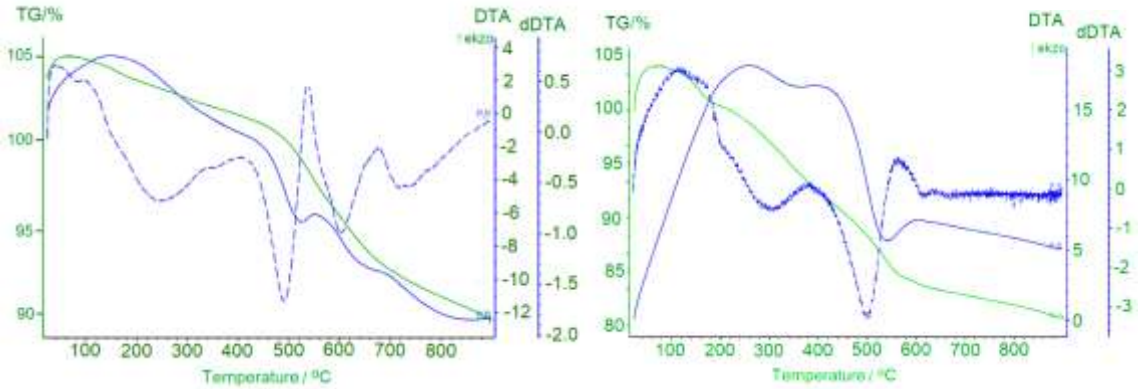

a) b)

Fig. 5. Thermograms of finely dispersed boehmite powders with ferrocene adsorbed at room temperature from an n-hexane solution, containing: a) 1.0 and b) 13.0 wt.% ferrocene and dried at 60°C for 2 hours.

As can be seen from the thermograms, a significant weight loss corresponding to dehydration-dehydroxylation of the samples was observed from 100 to 700◦C, which could be divided into two clearly visible stages. The first stage (from room temperature to 450◦C) is due to the desorption of physisorbed water molecules, n-hexane and thermo-oxidative

decomposition of most likely chemisorbed ferrocene. The second stage is due (450-600^{o}C) mainly to the release of water as a result of the transformation of boehmite into aluminum oxide (2AlOOH = Al_2O_3 + H_2O). Thermal decomposition of boehmite with adsorbed ferrocene occurs with the formation of an initially =Al-O-Fe(C_5H_5) structure on the surface of boehmite as a result of the reaction between ferrocene and the hydroxyls of the boehmite surface:

$$=Al\text{-}O\text{-}Fe(C_5H_5)\ =Al\text{-}OH + (C_5H_5)_2Fe \Rightarrow =Al\text{-}O\text{-}Fe(C_5H_5) + C_5H_6.$$

Calcination in air of a boehmite sample with adsorbed ferrocene is accompanied by a thermo-oxidative process, resulting in the formation of highly dispersed iron oxide structures that are not appear in X-ray diffraction patterns, but are clearly recorded in EPR spectra. Most likely, during calcination, part of the resulting highly dispersed iron oxide structures reacts with boehmite, forming solid solutions of $Al_{1-x}Fe_x)OOH$ based on boehmite at temperatures up to 600 °C and solid solutions of $Al_{2-x}Fe_xO_3$ at temperatures ≥ 600 °C.

Conclusion

The above studies and currently available literature data indicate that the thermochemistry of ferrocene and its derivatives applied to solid surfaces is insufficiently studied. In this paper, finely dispersed ferrocene is adsorbed by precipitation from a solution of n-hexane onto boehmite and the results of the study are presented using X-ray diffractometry, electron magnetic resonance and thermal analysis. Solid products of the interaction of ferrocene with boehmite during calcination in air have been identified.It is shown that with increasing calcination temperature, reactions of thermo-oxidative decomposition of ferrocene occur with the formation of iron oxides and stabilization of some iron ions in the form of Fe^{3+} ions in the boehmite structure and clusters of Fe^{3+} ions and/or FeO_x particles for samples with a low content of adsorbed ferrocene (<0.1 wt.% ferrocene) at a calcination temperature of up to 600°C and in the aluminum oxide structure at a calcination temperature above 600°C. For boehmite samples with a high content of supported ferrocene (>0.1 wt.%), calcination of boehmite samples with supported ferrocene is accompanied by the formation of iron oxide clusters, most likely Fe_2O_3. We believe that the obtained iron oxide structures are highly dispersed iron oxide formations that do not appear in X-ray diffraction patterns, but are quite clearly recorded in the EPR spectra.

Acknowledgments

The work was carried out with the financial support of the Ministry of Science and Education of the Azerbaijan Republic "Research and development in priority areas of catalysis and industrial chemistry. Preparation of oxide and polymer-based nanostructured catalysts, adsorbents and nanostructures."

References

1. Werner H. At least 60 years of ferrocene: the discovery and rediscovery of the sandwich complexes. *Angewandte Chemie*. 2012, Vol. **51(25)**, p. 6052-6058. https://doi.org/10.1002/anie.201201598
2. Phillips E.S., Ferrocenes: compounds, properties and applications. Chemical engineering methods and technology. *Nova Science Publishers*. 2011, 411 p.
3. Islam S., Wang F. A comparative study of energetics of ferrocenium and ferrocene. Preprints, (2018). https://doi.org/10.20944/preprints201808.0166.v1

4. Waldfried C., Welipitiya D., Hutchings C., De Silva H., Gallup G. A., Dowben P. A., Pai W., Zhang J., Wendelken J., Boag N. Preferential bonding orientations of ferrocene on surfaces. *J. Phys. Chem. B* 1997, Vol. **101(47)**, p. 9782-9789. https://doi.org/10.1021/jp972496l
5. Welipitiya D., Dowben P., Zhang J., Pai W., Wendelken J. The adsorption and desorption of ferrocene on Ag(100). *Surface Science*, 1996, Vol. **367**, p.20–32. https://doi.org/10.1016/S0039-6028(96)00855-2
6. Welipitiya D., Green A., Woods J.P., Dowben P.A., Robertson B.W., Byun D., Zhang J. Ultraviolet and electron radiation induced fragmentation of adsorbed ferrocene. J. *Applied Physics*, 1996, Vol. **79**, p. 8730–8734. https://doi.org/10.1063/1.362474
7. Ormaza M., Abufager P., Bachellier N., Robles R., Verot M., Le Bahers T., Bocquet M.-L., Lorente N., Limot L. Assembly of ferrocene molecules on metal surfaces revisited. *The Journal of Physical Chemistry Letters* 2015, Vol. **6**, p. 395–400. https://doi.org/10.1021/jz5026118
8. Paul R., Reifenberger R.G., Fisher T.S., Zemlyanov D.Y. Atomic layer deposition of FeO on Pt(111) by ferrocene adsorption and oxidation. *Chemistry of Materials*, 2015, Vol. **27**, p. 5915–5924. https://doi.org/10.1021/acs.chemmater.5b01778
9. Reimers J.R., Wang Y., Kosov D.S. Decomposition of ferrocene on Pt(111) and its effect on molecular electronic junctions. *Journal of Physical Chemistry C*, 2019, Vol. **123(25)**, p. 15569-15574. https://doi.org/10.1021/acs.jpcc.9b02628
10. Nigar S., Wang H., Imtiaz M., Yu J., Zhou Z. Adsorption mechanism of ferrocene molecule on pristine and functionalized graphene. *Applied Surface Science*, 2019, Vol. **481**, p. 1466-1473. https://doi.org/10.1016/j.apsusc.2019.03.222
11. Woodbridge C., Pugmire D., Johnson R., Boag N., Langell M. HREELS and XPS Studies of Ferrocene on Ag (100). *J. Phys. Chem B*, 2000, Vol. **104**, p. 3085-3093. https://doi.org/10.1021/jp993235+
12. Quardokus R.C., Wasio N.A., Forrest R.P., Lent C.S., Corcelli S.A., Christie J.A., Henderson K.W., Kandel S.A. Adsorption of diferrocenylacetylene on Au(111) studied by scanning tunneling microscopy. *Phys. Chem. Chem. Phys.*, 2013, Vol. **15**, p. 6973-6981. https://doi.org/10.1039/C3CP50225B
13. Heinrich B., Limot L., Rastei M., Iacovita C., Bucher J., Djimbi D.M., Massobrio C., Boero M. Dispersion and localization of electronic states at a ferrocene/Cu (111) interface. *Phys. Rev. Lett.* 2011, Vol. **107**, 216801. https://doi.org/10.1103/PhysRevLett.107.216801
14. Fan L., Zhang Q., Wang K., Li F., Niu L. Ferrocene functionalized graphene: preparation, characterization and efficient electron transfer toward sensors of H_2O_2. *J. Mater. Chem.* 2012, Vol. **22**, p. 6165-6170. https://doi.org/10.1039/C2JM15411K
15. Larik F.A., Saeed A., Fattah T.A., Muqadar U., Channar P.A. Recent advances in the synthesis, biological activities and various applications of ferrocene derivatives. *Appl. Organomet. Chem.* 2017, Vol. **31**, 3664. https://doi.org/10.1002/aoc.3664
16. Hall J.N., Chapovetsky A., Kanbul U., Kim Y.L., McCullough K.E., Syed Z.H., Johnson Ch.S., Ferrandon M.S., Liu C.A., Kropf J., Delferro M., Kaphan D.M. Oxidative Grafting for Catalyst Synthesis in Surface Organometallic Chemistry. *ACS Appl Mater Interfaces*, 2023, Vol. **15(46)**, p. 53498-53514. https://doi.org/10.1021/acsami.3c12656
17. Guan E., Fang Ch.-Y., Yang D., Wang L., Xiao F.-Sh., Gates B.C. Supported cluster catalysts synthesized to be small, simple, selective, and stable. *Faraday Discussions*, 2018, Vol. **208**, p. 9-33. https://doi.org/10.1039/C8FD00076J
18. Samudrala K.K., Conley M.P. Effects of surface acidity on the structure of organometallics supported on oxide surfaces. *Chem. Commun.*, 2023, Vol. **59**, p. 4115-4127. https://doi.org/10.1039/D3CC00047H
19. Bhattacharjee A., Rooj A., Roy D., Roy M. Thermal Decomposition Study of Ferrocene [$(C_5H_5)_2Fe$]. *Hindawi Publishing Corporation Journal of Experimental*

Physics, 2014, Article ID 513268, 8 pages; http://dx.doi.org/10.1155/2014/513268

20. Rustamova A.I., Gurbanov Z.G., Mammadova Z.M., Osmanova S.N., Guluzade A.Kh., Mammadov A.N., Ismailov E.H. Thermal stability and thermodynamics of pyrolysis of mono-,bi-,and trinuclear carbinol derivatives of ferrocene. *Chemical Problems*, 2023, Vol. **21(3)**, p. 251-261. https://chemprob.org/wp-content/uploads/2023/08/251-261.pdf
21. Chabaud B., Bonnet H., Lartia R., Van Der Heyden A., Auzély-Velty R., Boturyn D., Coche-Guérente L, Dubacheva G.V. Influence of Surface Chemistry on Host/Guest Interactions: A Model Study on Redox-Sensitive β-Cyclodextrin/Ferrocene Complexes. *Langmuir*, 2024, Vol. **40(9),** p. 4646-4660. https://doi.org/10.1021/acs.langmuir.3c03279
22. Sakurai M. On-surface synthesized magnetic nanoclusters of ferrocene derivatives. *Chem. Synth.*, **2024**, Vol. **4**, p. 42. http://dx.doi.org/10.20517/cs.2023.76
23. Kundu S., Sarkar T., Ghorai G., Sahoo P.K., Al-Ahmadi A.A., Alghamdi A., and Bhattacharjee A. Reaction Atmosphere-Controlled Thermal Conversion of Ferrocene to Hematite and Cementite Nanomaterials-Structural and Spectroscopic Investigations. *ACS Omega*, 2024, Vol. **9(21),** p. 22607-22618. https://doi.org/10.1021/acsomega.3c10332
24. Samantaray M.K., Mishra S.K., Saidi A., Basset J.-M. Surface organometallic chemistry: A sustainable approach in modern catalysis. *Journal of Organometallic Chemistry*, 2021, Vol. **945**, 121864. https://doi.org/10.1016/j.jorganchem.2021.121864
25. Samantaray M.K., Pump E., Bendjeriou A., Sedjerari D'Elia V., Pelletier J.D.A., Guidotti M., Psaro R., Basset J.M. Surface organometallic chemistry in heterogeneous catalysis. *Chem. Soc. Rev.*, 2018, Vol. **47**, p. 8403-8437. https://doi.org/10.1039/C8CS00356D
26. Scott S.L., Basset J.M., Niccolai G.P., Santini C.C., Candy J.P., Lecuyer C., Quignard F., Choplin A. Surface organometallic chemistry a molecular approach to surface catalysis. *New J. Chem.*, 1994, Vol. **18**, p.115-122. https://doi.org/10.1007/978-94-009-2971-5
27. Rouge P., Garron A., Norsic S., Larabi Ch., Merle N., Delevoye L., Gauvin R.M., Szeto K.C., Taoufik M. A smarter approach to catalysts by design: Combining surface organometallic chemistry on oxide and metal gives selective catalysts for dehydrogenation of 2,3-dimethylbutane. *Molecular Catalysis*, 2019, V. **471**, p. 21-26. https://doi.org/10.1016/j.mcat.2019.04.011
28. Copéret Ch., Comas-Vives A., Conley M.P., Estes D.P., Fedorov A., Mougel V., Nagae H., Núñez-Zarur F., Zhizhko P.A. Surface Organometallic and Coordination Chemistry toward Single-Site Heterogeneous Catalysts: Strategies, Methods, Structures, and Activities. *Chem. Rev*. 2016, Vol. **116**, p. 323−421324. https://doi.org/10.1021/acs.chemrev.5b00373
29. Coperet C., Chabanas M., Saint-Arroman R.P., Basset J.M. Homogeneous and heterogeneous catalysis: bridging the gap through surface organometallic chemistry. *Angew. Chem. Int. Ed.*, 2003, Vol. **42**, p. 156-181 https://doi.org/10.1002/anie.200390072
30. Boumaza A., Favaro L., Ledion J., Sattonay G., Brubach J.B., Berthet P., Huntz A.M., Roy P., Tetot R. Transition alumina phases induced by heat treatment of boehmite: An X-ray diffraction and infrared spectroscopy study. *J. Solid State Chemistry*, 2009, V. **182(5)**, p. 1171-1176. https://doi.org/10.1016/j.jssc.2009.02.006
31. Can M.M., Coşkun M., Fırat T. A comparative study of nanosized iron oxide particles; magnetite (Fe_3O_4), maghemite (γ-Fe_2O_3) physical series «Nuclei, Particles, Fields», issue 3.The structure and EPR and hematite (α-Fe_2O_3), using ferromagnetic resonance. *Journal of Alloys and Compounds*. 2012, V. **542**, p. 241–247. https://doi.org/10.1016/j.jallcom.2012.07.091
32. Hseih C.T., Huang W.L., Lue J.T. The change from paramagnetic resonance to ferromagnetic resonance for iron

33. nanoparticles made by the sol–gel method. *J. of Physics and Chemistry of Solids*. 2002, V. **63**, p. 733–741. https://doi.org/10.1016/S0022-3697(01)00222-0
34. Jahagirdar A.A., Dhananjaya N., Monika D.L., Kesavulu C.R., Nagabhushana H., Sharma S.C., Nagabhushana B.M., Shivakumara C., Rao J.L., Chakradhar R.P.S. Structural, EPR, optical and magnetic properties of α-Fe_2O_3 nanoparticles. *Spectrochimica Acta Part A: Molecular and Biomolecular Spectroscopy*. 2013, V.**104**, p. 512–518; https://doi.org/10.1016/j.saa.2012.09.069
35. Alphonse P., Courty M.. Structure and thermal behavior of nanocrystalline boehmite. *Thermochimica Acta*, 2005, Vol. **425(1-2)**, p. 75-89. https://doi.org/10.1016/j.tca.2004.06.009